Impact of groundwater flow on permafrost degradation: implications for transportation infrastructures

I. de Grandpré[1,2], D. Fortier[1,2,3] and E. Stephani[2,3,4]
[1] Département de Géographie, Université de Montréal, Québec, Canada
[2] Centre d'études nordiques, Université Laval, Québec, Canada
[3] Institute of Northern Engineering, University of Alaska Fairbanks, USA
[4] Department of Civil and Environmental Engineering, University of Alaska Fairbanks, USA

ABSTRACT
The Alaska Highway is the main terrestrial link between Alaska and the contiguous USA. Since its rehabilitation in the past decades the road has subsided in response to the degradation of the underlying ice-rich permafrost. At the study site near Beaver Creek (Yukon) the embankment material now intersects the natural groundwater table. It is suggested that water flow under the road proceeds along preferential flow paths essentially located within thawed embankment material. Measurements of water temperature indicate that the water is progressively loosing heat as it flows under the road. We propose that this energy transfer to the surrounding ground contributes to the degradation of the underlying permafrost through various processes of convective and conductive heat transfer.

RÉSUMÉ
L'Alaska Highway est le lien principal qui relie l'Alaska au reste des États-Unis. Suite à sa réhabilitation au cours des dernières décennies la route s'est enfoncée en réponse à la dégradation du pergélisol riche en glace sous-jacent. Au site d'étude près de Beaver Creek (Yukon) le matériel de remblai intercepte maintenant le réseau d'écoulement naturel. L'écoulement sous la route s'effectue probablement le long de chenaux d'écoulement préférentiels situés dans le matériel de remblai dégelé. Les mesures de température de l'eau indiquent qu'elle perd de la chaleur lorsqu'elle s'écoule sous la route. Nous proposons que ce transfert de chaleur entre l'eau et le sol encaissant contribue à la dégradation du pergélisol sous-jacent via divers processus de transfert de chaleur conductif et convectif.

1   INTRODUCTION

In the present global warming trend temperatures are expected to increase twice as fast in high latitude (i.e. Arctic) than in mid latitude regions (Overpeck et al. 1997; IPCC 2007; Wedler and Shulski 2009). Permafrost warming is a reality in several northern areas and has been affecting the north-western portion of North America for a few decades now (Zhang et al. 2008). This warming alters the thermal state of the permafrost and promotes permafrost degradation. This degradation can also occur as the result of other natural processes such as thermo-erosion, thicker snow cover or changes in vegetation (Serreze et al. 2000; Hinzman et al. 2005; Smith et al. 2005; Jin et al. 2006; Fortier et al. 2007; Zhang et al. 2008).

When the ground is ice-rich, thawing of permafrost usually induces thaw-settlement, ground subsidence, surface disturbance and changes in drainage conditions. Transportation infrastructures built on permafrost are particularly sensitive to permafrost stability (Allard et al. 2007). Melting of ground ice and consolidation of thawed soil promote road embankment subsidence and the development of cracks, potholes and depressions in the road pavement (Figure 1) (Quingbai et al. 2002).

A natural permafrost warming trend can be exacerbated by construction operations (e.g. soil compaction, destruction of the vegetation cover) (Wu et al. 2002), embankment geometry and snow maintenance operations (snow accumulation on side slope) or changes in material properties (e.g. pavement albedo vs natural ground) (Kondratiev 2009). Linear transportation infrastructure embankments built on permafrost often intersect the natural drainage network. Usually culverts are inserted in embankments to drain the main streams intersected by the infrastructure and bridges are built for river crossing. Groundwater flow paths however are rarely taken into account in the design of embankments and the impact of groundwater flow on permafrost degradation is still poorly known (Woo et al. 2008).

Figure 1. Depressions in the road (black arrows) at the study site are outlined by water accumulation during a rain event. The road is 15 m wide.

We report in this paper observations of groundwater flow and signs of road subsidence under a segment of the Alaska Highway. Because the active layer at the time of observation (June: 2.5 m deep) was still located in the embankment (4 to 6 m thick) and therefore not deep enough to cause permafrost thawing under the road, we propose that ground ice melting and observed road subsidence were related to heat transfers by groundwater flowing under the road. We designed a methodology to measure groundwater flow and water temperature using a network of piezometers and pressure-temperature sensors.

The objectives of the research project are: 1) to estimate the potential groundwater flowpaths under a road embankment; 2) to measure water temperature as it flows under the road embankment.

2. STUDY SITE

The site is located in the zone of widespread discontinuous permafrost along a segment of the Alaska Highway near Beaver Creek, Yukon (Figure 2A: 62°20' N, 140°50' W) (Rampton 1971; Scudder 1997). The Beaver Creek area is characterized by a cold continental climate with short, warm, dry summers and long, cold winters (Rampton 1971; Scudder 1997; Ogden 2006). The mean annual air temperature is -5.5°C and four months of the year have a mean air temperature above 0°C. The mean annual precipitation is 416.3 mm. Snow precipitations begin in September and the snowmelt period usually begins in April (Environment Canada, 2009). The vegetation is muskeg taiga with stunted spruce, shrubs, tussocks and mosses (Scudder 1997). Surficial deposits at the study site comprise a layer of poorly-decomposed organic matter and wood fragments overlying well-decomposed cryoturbated peat mixed with silt and tephra grains. This organic unit rests on several meters of coarse silt. At the location of the study site the embankment is sub-perpendicular to the local slope and thus intersects the natural drainage network (Figure 2B).

Since its construction the road has subsided in response to the degradation of the underlying ice-rich permafrost and currently requires recurrent maintenance and fills operations (Remchein et al. 2009). Excavations done in April 2008 to remove a berm on the side of the road revealed the presence of saturated taliks (unfrozen zone within the permafrost) in and under the road embankment (Stephani et al. 2008). These taliks are located in coarse embankment material and in the underlying fine-grained natural ground (decomposed organic matter mixed with alluvial sandy silt).

3. METHODOLOGY

3.1 Groundwater flow measurement

A network of 25 piezometers was installed at the study site, 11 on the northern side of the road (Figure 3) and 14 on the southern side. On each side of the embankment, two rows of piezometers were installed, one in the undisturbed natural ground and one at the toe of the embankment where the ground comprises a mixture of embankment material and a small and variable amount of reworked peat and silt. Six pore water pressure
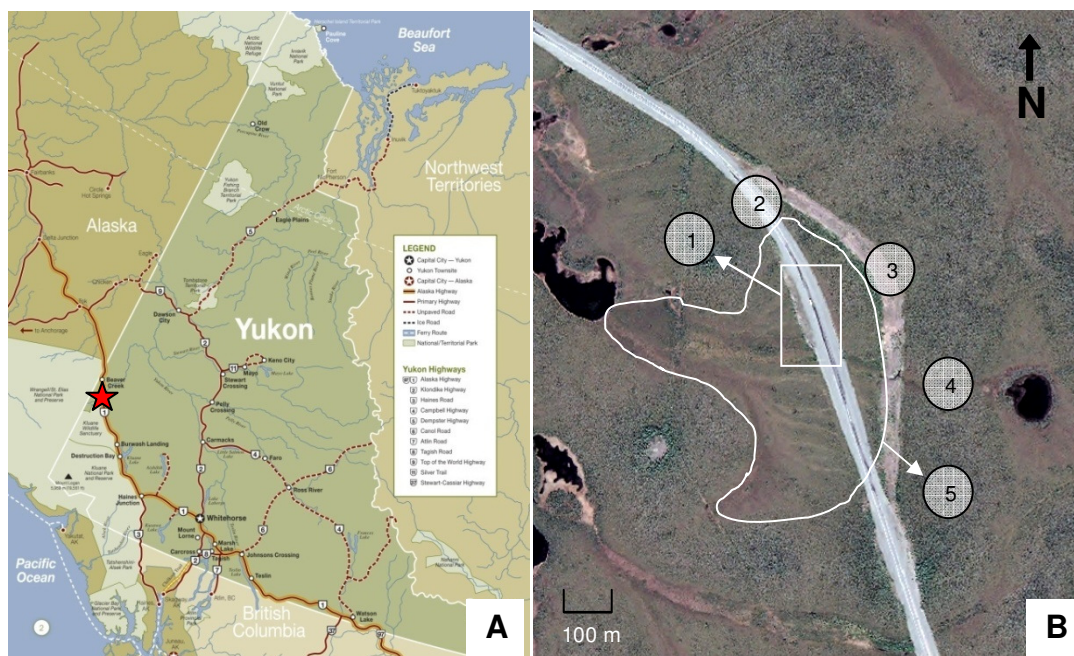

Figure 2. Localization of the study site (62°20' N, 140°50' W) **A**. Map of Yukon Territory, Canada (www.gov.yk.ca) **B**. Satellite image (QuickBird) of the study site took on June 14, 2006.1. Inset: groundwater measurements location (piezometers and pressure sensors) 2. Alaska Highway 3. Former Alaska Highway alignment 4. Stream 5. The line shows an area with a vegetation pattern (lighter grey) aligned with the direction of groundwater flow.

transducers (Onset Hobo U20 water logger) equipped with temperature sensor and datalogger were installed in six piezometers at the potential location of preferential flowpaths where seepage and outflow were observed on each side of the road.

The piezometers were installed in 2008 in holes made with a portable core drill. The holes extend down to the bottom of the active layer (top of permafrost). Hydrostatic pressure at the bottom of the piezometers and water temperature were measured and recorded every hour by automatic loggers. The accuracy of measured water levels is about 2.1 mm (0.02 KPa). Hydrostatic pressure data from piezometers were corrected for variations in atmospheric pressure measured on site using the Hoboware Pro™ software. After corrections, hydrostatic pressure data were converted to water level data (cm of water in piezometer).

Additional water level and temperature measurements were done manually in the field in October 2008 and five times between June and August 2009. These data are used to validate automated measurements and to obtain a snapshot of groundwater flow paths at the time of measurement.

Figure 3. Piezometer network (wooden stakes under arrows) on the northern side of the road. The white horizontal and vertical pipes in the background are mitigation measures to control permafrost degradation (see Fortier et al. for details in these proceedings)

3.2 Microtopography and piezometer location

The local microtopography was characterized using a combination of optical level, laser level and compass. Surface elevation at piezometer location was obtained by optical reading (Zeiss Ni2 level) with a setting accuracy of 5 mm and a leveling accuracy of 0.7 mm per 1000 m. A laser leveling (Bushnell Rangefinder 1500) with a precision of about 1 m was used to obtain the horizontal distance between piezometers. Slope and azimuth between piezometers were obtained by compass (two degrees of resolution). Compass readings (α) were corrected with a magnetic declination of 22°E (National Geophysical Data Center). Three transects connecting the piezometers across the road were surveyed using optical level, compass and measuring tape. Transects and piezometers were georeferenced to a geodesic point located at about 100 m from the study site.

We used Differential Global Positioning System (DGPS) (Trimble GPS Pathfinder Pro XRS with a TSC1 data collector) to validate data position in x and y with a precision of about 50 cm.

Piezometer and transect positions were imported into a Geographic Information System (GIS) and laid over a georeferenced Quickbird satellite image of the study site. Elevation data collected by optical level were used together with water level in piezometer to estimate the preferential flow paths at the study site.

3.3 Stratigraphy

We used a portable corer to collect soil sample from the surface to the base of the active layer beside each piezometer and along three transects. The stratigraphy at the study site has been determined by the detailed description of assemblages of cryostructures, sediments, and organic matter (cryofacies) within cores retrieved in the natural ground adjacent to the road and under the road berm (Stephani et al. 2008).

3.4 Temperatures of the road embankment and natural ground

Temperatures were measured with thermistor cables installed in 2008 in the southern side slope of the road in embankment material (about 4 m thick) and in the underlying natural ground (about 4 m to 16 m under the surface). Two cables installed at the centerline of the road are located at about 180 m east and 100 m west of the piezometer network location. Temperatures are recorded at various depths (0,1 m, 1.5 m, 1.8 m, 2.1 m, 2.5 m, 3 m, 3.5 m, 3.9 m, 4.3 m, 4.5 m, 6 m, 7.5 m, 9 m, 11 m,13 m, 16 m) every four hours since October 2008.

4. RESULTS

4.1 Microtopography

The site where groundwater flow was measured covers an area of about 100 m². The northern side of the road is about 2.5 m higher than the southern side. The slope gradient is about 2.5% and is aligned perpendicular to the road. The road was built on about 4 to 6 m of embankment material (sand and gravel with a fraction of silt) laid over the natural ground. Figure 4 shows the emplacement of piezometers and automatic water level/temperature loggers (PWPT). Three transects were used to represent the elevation profile of the road and the natural ground and to evaluate potential flow paths under the embankment.

4.2 Local stratigraphy

The typical stratigraphy of the active layer at the study site comprises a layer of peat at the surface (between 30 and 45 cm thick) covering cryoturbated peaty silt with tephra (volcanic ashes).
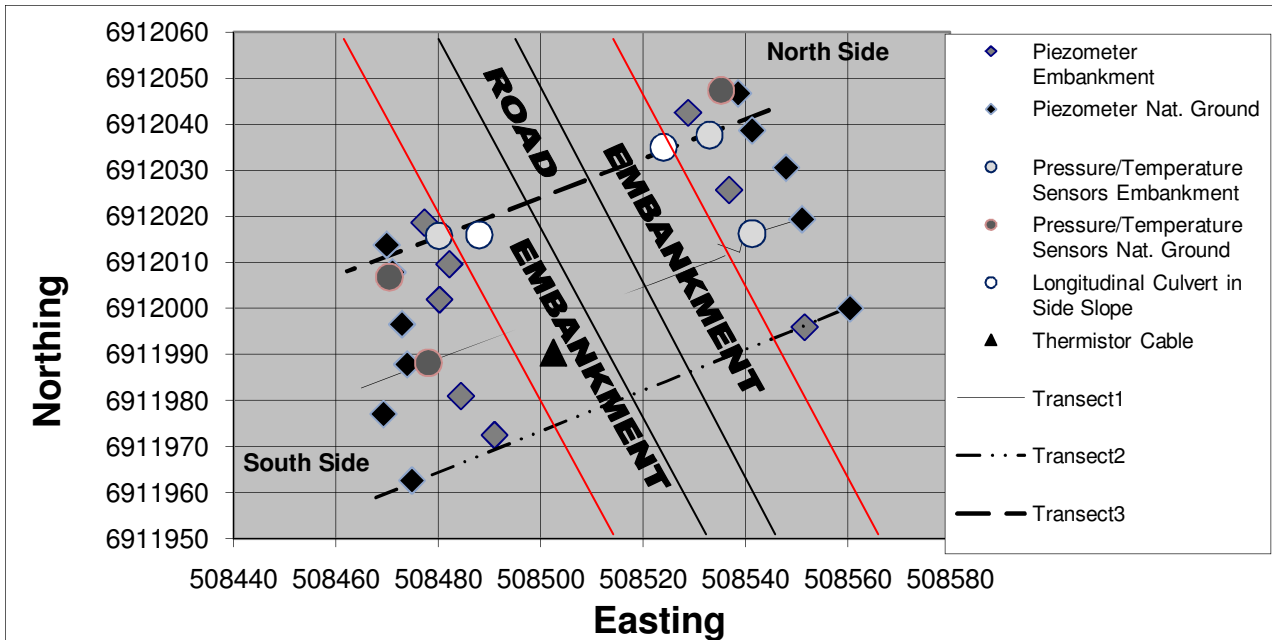
Figure 4. Research design. The piezometers are located on each side of the road at the toe of the embankment (grey diamond) and in the adjacent natural ground (black diamond). Automated pressure and temperature sensors installed in piezometers are located at the toe of the embankment (light grey circles) and in the natural ground (dark gray circles). White circles show the location of longitudinal culvert in the side slope. Three transects were used to evaluate potential flow paths under the road.One thermistors cables is installed in the side slope of the embankment and two others are installed under the centre line of the road at about one hundred meters on each side of the piezometers network (not shown on figure)

Drilling operations indicate that the embankment at the centerline of the road is about 6 m thick. On the road side slopes the embankment is about 4 m thick and the material is plastic down to about 3 m into the natural ground. It is not known if the material was in a cryotic state (below 0℃ but plastic due to its high unfrozen water content) or actually thawed. The grab samples collected from this layer (no core) indicate that the material was probably composed of thawed embankment material that has partially sunk, and thawed saturated peaty silt. This mixture of embankment material and natural ground is presumably similar to the material at the toe of the embankment where berms were removed in 2008. Below the 3 m thick unfrozen zone (or in a cryotic state) there is a layer of ice rich peaty silt down to about 6.5 m under the natural ground surface. This layer correspond to unit 2 describes in Stephani et al. (2008). An ice-rich diamicton (unit 3) is observed from about 6.5 m deep (extent depth unknown).

Figure 5 shows a schematic cross-section of the road and underlying natural ground at the study site. As a result of permafrost degradation, the road embankment has subsided in the thawed natural ground (peat and silt) and the embankment material is now located under the natural ground surface and therefore intersects the water table and groundwater flow paths.

4.3 Permafrost table

In the natural ground the permafrost table is located at a depth of about 50 cm and at about 80cm in the reworked ground (mixture of embankment material and natural ground) at the toe of the embankment. According to thermistor cables data (installed in the side slope) and coring data, the permafrost table is located at about 6 m under the slope. There are no thermal or coring data available for the northern side of the road but the permafrost table is presumably located at the same depth (or a little higher due to exposition). Figure 5 shows a linear interpolation of the permafrost table under the road assuming symmetry between the side slopes.

4.4 Water table elevation

The water table is following the topography and is about 2.5 m higher on the northern side of the road than on the southern side. When thawed, the natural ground was generally saturated except in the highest piezometers located on the northern side of the road (piezometers 4 to 8). The linear interpolation of water table elevations under the road (Figure 5) shows that the embankment material is intercepting the water table under the central line of the road and that the water is flowing from the northern side of the road to the southern side according to the local hydraulic gradient. Observations of water infiltration in longitudinal culverts located in the side slopes on both

side of the embankment confirmed groundwater flow under the road.

4.5 Road and ground temperature

Figure 6 shows temperature data recorded by pore water pressure and temperature sensors from June to October 2009 on both side of the road and under the road side slopes along a transect. Water temperatures on the northern side of the road are higher than on the southern side by 2 to 4 °C.

Temperature data from thermistor cables between 0.1 m and 3.5 m show very concordant trends (Figure 7A, B). Temperatures profiles at depths of 3.9 and 4.5 m are similar and stay in isothermal condition very close to 0 °C from June 2009 to January 2010. Temperature profile at depth of 4.3 m has less amplitude and stays in isothermal condition around 0 °C for four months longer. Temperatures at a depth of 6m and lower remained under 0 °C all year (7D). Note that temperatures in the depth interval 6 to 16 m are decreasing with depth.

4.6 Road subsidence

During the summer 2008 and 2009, measurements of depressions on the road surface indicate that road subsidence was in the order of 30 cm each summer.
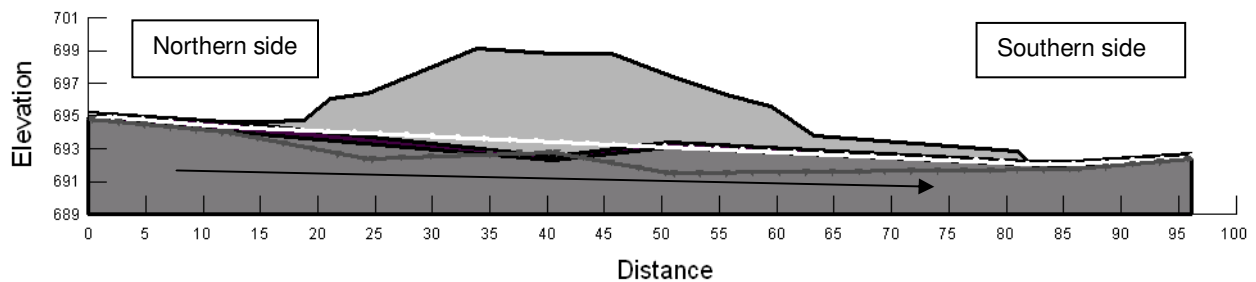

Figure 5. Cross-sectional transect of the road embankment and the underlying natural ground. Light grey: embankment material, black: peat, dark grey: silt. The upper dotted line represents an interpolation of water table and the lower one is an interpolation of the permafrost table. The arrow shows the general direction of groundwater flow.
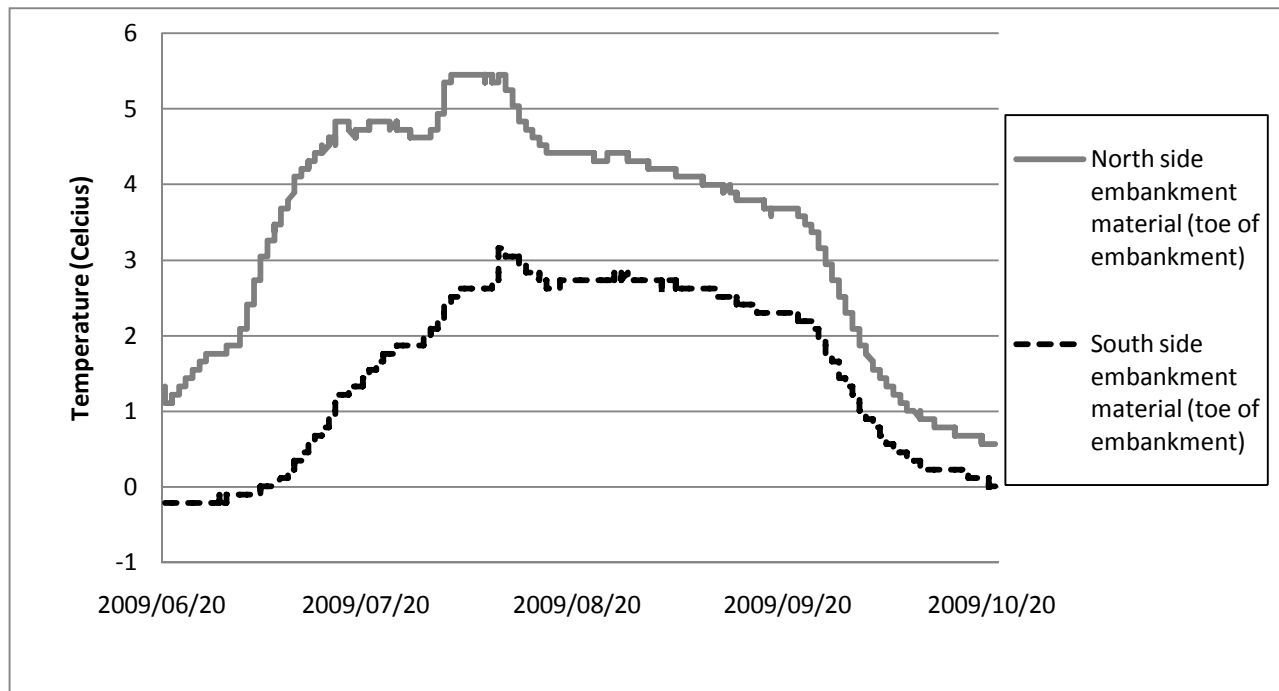

Figure 6. Water temperature profiles along transect 3 (Figure 4) between June and August 2009. Note the difference of water temperature between the northern and southern sides of the road, indicating that water is transferring heat to the surrounding ground as it flows under the embankment.
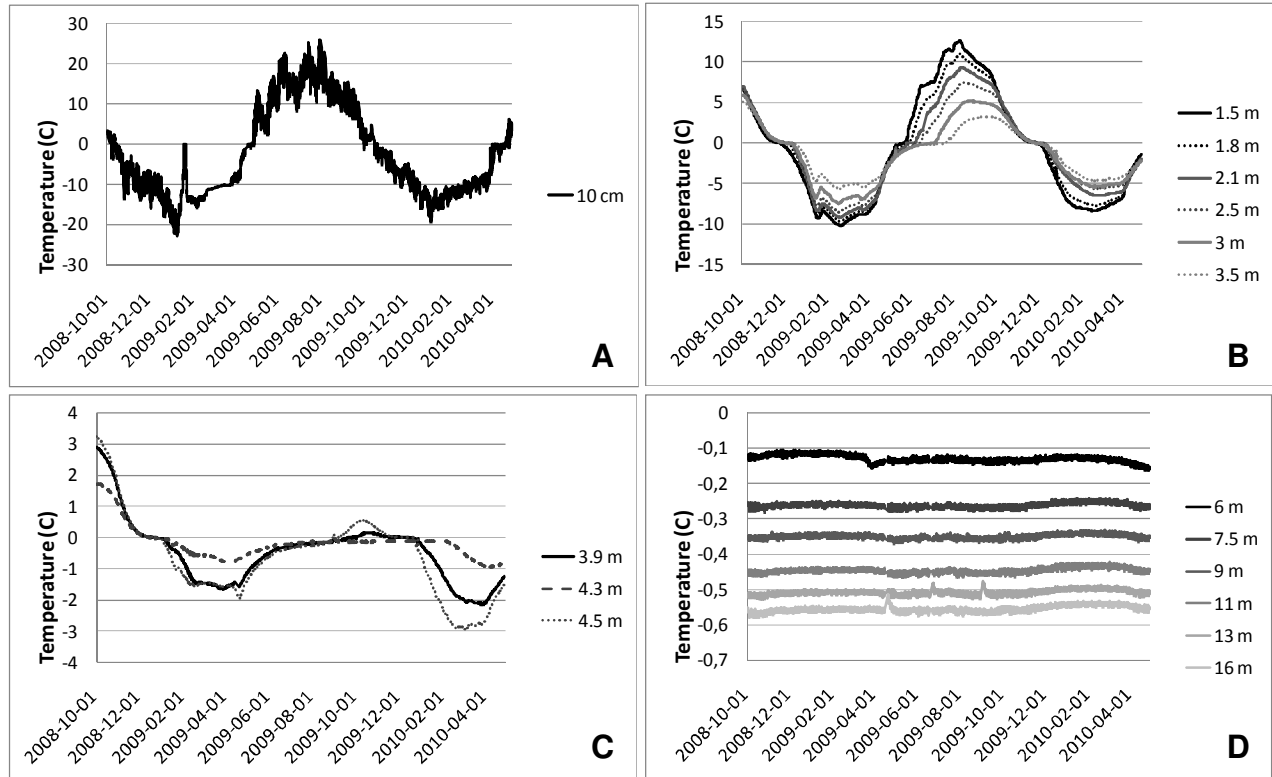
Figure 7. Temperatures recorded by thermistors cable at various depths between October 2008 and April 2010. A: Depth of 0.1m. B: Embankment (1.5 to 3.5 m). C: Interface embankment-natural ground (3.9 to 4.5 m). D: natural ground (6 to 16 m).

5. DISCUSSION

Road construction and maintenance operations may induce heat flow to the underlying ground (e.g. soil compaction, snow accumulation on side slope, pavement albedo or thin berms) and can have an important thermal impact on permafrost. In ice-rich permafrost, heat flow will initiate and promote melting of ground ice, thaw settlement and road subsidence. As the road subsides over the years, the embankment material will eventually intercept the water table and groundwater flowpaths where the road is intersecting the natural drainage pattern and local hydraulic gradient.

At the study site field observations suggested that groundwater flow occurs under the road. These observations were confirmed by water table elevation measurements. We propose that groundwater flow likely proceeds within unfrozen zones (taliks) located under the side slopes and the central portion of the road. Thermistor cables indicate that the temperature between 4.5 and 7 m are very close to 0°C. At this temperature, the unfrozen water content of silt is very high and allows groundwater flow. The hydraulic conductivity of embankment material is about three orders of magnitude larger than silt. In the summer, groundwater flow first proceeds at the toe of the embankment as the active layer is progressing in the embankment material. Groundwater helps to melt ice in the porosity of the underlying embankment material therefore enlarging the flow paths. Once the ice is melted

in the embankment material, water can access the underlying silt and flow through it due to its high unfrozen water content. However, the very low hydraulic conductivity of silt likely prevents high groundwater flow discharge.

As water flows under the road, heat is transferred to the surrounding ground. Convective heat transfer due to groundwater flow in embankment material promotes rapid heat flow to the underlying silt. This changes the boundary conditions at the embankment/silt interface under the road compared to zones where groundwater flow under the road is absent.

We assume that water flow in silt is slow and that conducto-convective heat transfers prevail. Heat flow to the permafrost (likely in a cryotic state down to at least -0.2°C) promotes ice melting. Latent heat effects associated with ice melting likely explain the thermal state of the permafrost below (cooling with depth).

Repetition of groundwater flow under the road over the years increases permafrost degradation and explains the important depressions and cracks observed in the road surface at the study site. Observations of water flow in October 2009 when the upper portion of the active layer was frozen suggest that this process remains active for extensive periods of the year.

6. CONCLUSION

(1) There is groundwater flow under the road at the study site. Water flow proceeds along preferential flowpaths in thawed embankment material and is accelerated by the presence of taliks.

(2) Water is transferring 2 to 4°C to the surrounding material as it passes under the road during the groundwater flow season. This heat is transferred to the underlying permafrost and leads to permafrost degradation.

(3) Groundwater flow is a process underestimated in dynamics of permafrost degradation. Because of accelerated embankment damages related to convective heat transfer, groundwater flow should be taken into account in the road design.

7. AKNOWLEDGEMENT

8. REFERENCES

Allard, M., Calmels, F., Fortier, D., Laurent, C., L'Hérault, E., and Vinet, F 2007. L'impact du réchauffement climatique sur les aéroports du Nunavik: caractéristiques du pergélisol et caractérisation des processus de dégradation des pistes, *Rapport à Ouranos,* Université Laval, Centre d'études nordiques, Ressources Naturelles Canada et Transports Québec, 192 p.

Environment Canada 2009. *National Climate Data and Information Archive* www.climat.meteo.gc.ca

Fortier, D., Allard, M. and Shur, Y. 2007. Observation of Rapid Drainage System Development by Thermal Erosion of Ice Wedges on Bylot Island, Canadian Arctic Archipelago, *Permafrost and Periglacial Process* **18**: 229–243

Fuller, T. and Jackson, L. 2004. Quaternary Geology of the Yukon Territory*, Yukon Geological Survey,* p.1-3

Hinzman, L., et al. (2005), Evidence and implications of recent climate change in northern Alaska and other Arctic regions*, Climatic Change* **72**: 251–298

Jin, H, Zhao, L., Wang, S. and Jin, R 2006. Thermal regimes and degradation modes of permafrost along the Qinghai-Tibet Highway, *Science in China Series D: Earth Sciences* **49**(11): 1170—1183.

Kondratiev, V.G. 2009. Geocryological Problems Associated with Railroads and Highways*, Proceeding of 9th International Permafrost Conference*, Fairbanks, p. 977-982

Mackay, J. 1983. Downward water movement into frozen ground, western arctic coast, Canada*, Earth sciences* **20** 120-134

Ogden, A. 2006. Climate, climate change variability and climate change in the Southwest Yukon, *Northen climate Exchange,* p.6

Overpeck, J., Hughen, K., Hardy, D., Bradley, R., Case, R., Douglas, M., Finney, B., Gajewski, K., Jacoby, G., Jennings, A., Lamoureux, S., Lasca, A., MacDonald, G., Moore, J., Retelle, M., Smith, S., Wolfe, A. and Zielinski, G. 1997. Arctic Environmental Change of the Last Four Centuries*, Science* **278**: 1251

Quingbai, W., Yuanlin, Z and Yonzhi, L 2002. Evaluation model of permafrost thermal stability and thawing sensibility under engineering activity*, Cold Regions Science and Technology* **34**: 19–30

Rampton, V. 1971. Late Pleistocene Glaciations of the Snag-Klutlan Area,Yukon Territorv*, Gelogical Survey of Canada,* p. 10-13

Remchein, D., Fortier, D., Dore, G., Stanley, B., Walsh, R. 2009. Cost and Constructability of Permafrost Test Sections Along the Alaska Highway, Yukon, *Proceedings of Transport Association of Canada Annual Conference*, Vancouver, October 2009

Scudder, G. 1997. *Environment of Yukon* in Danks and J.A. Downes (Eds.), *Insects of the Yukon*, Biological Survey of Canada (Terrestrial Arthropods), p. 13-57

Serreze, M. Walsh, J., Chapin,F., Osterkamp, T., Dyurgerov, M., Romanovsky, V., Oechel, W., Morison, J., Zhang, T. and Barry, R. 2000. Observational evidence of recent change in the northern high-latitude environment*, Climatic Change* **46:** 159–207

Smith, S., Burgess, M., Riseborough, D. and Nixon, F. 2005. Recent Trends from Canadian Permafrost Thermal Monitoring Network Sites*, Permafrost and Periglacial Process* **16**: 19–30

Stephani, E., Fortier, D. Shur, Y., Doré, G., Stanley, B. 2008. Preservation of the Alaska Highway, *Proceedings, Ninth International Conference on Permafrost*, Fairbanks, U.S.A., 299-300

Wendler, G. and Shulski, M. (2009), A Century of Climate Change for Fairbanks Alaska*, Arctic* **62**: 295–300

Woo, M. Kane, D., Carey, S. and Yang, D. 2008. Progress in Permafrost Hydrology in the New Millennium*, Permafrost and Periglacial Process* **19**: 237–254

Wu, Q., et al. 2002. A Review of Recent Frozen Soil Engineering in Permafrost Regions along Qinghai-Tibet Highway, China*, Permafrost and Periglacial Processes* **13**: 199–205

Zhang, Y., Chen, W. and Riseborough,D. 2008. Transient projections of permafrost distribution in Canada during the 21st century under scenarios of climate change*, Global and Planetary Change* **60:** 443–456